



## An Approach to Preliminary Design of a Quadrotor Cargo UAV

Fikret Kamil Corbaci \*<sup>1</sup>, Yunus Emre Dogan<sup>2</sup>

<sup>1</sup>Ankara Yıldırım Beyazıt University, Aeronautics and Astronautics Engineering Department, Ankara/ Turkey  
[fikretkamil.corbaci@gmail.com](mailto:fikretkamil.corbaci@gmail.com) - 0000-0002-0499-8694

<sup>2</sup>Ankara Yıldırım Beyazıt University, Mechanical Engineering Department Ankara/ Turkey  
[ynsemrd@gmail.com](mailto:ynsemrd@gmail.com) - 0009-0005-6250-0523



### Abstract

Unmanned aerial vehicles (UAV) are widely used in many different application areas today. UAVs are very cheaper than the other aerial platform and also their give opportunity to users in operating flexibility. It can be mentioned that the cargo transportation of UAV application area has high potential to grow. Compared to traditional highway delivery methods, cargo drones can offer cost savings by eliminating the need for human drivers, reducing fuel consumption, and optimizing delivery routes. Cargo drones can revolutionize the e-commerce industry by offering same-day or even same-hour delivery options. This can improve customer satisfaction, reduce shipping costs, and enable businesses to expand their operations. The main purpose of the study is to develop a preliminary design method for a quadrotor Cargo UAV to be used for cargo transportation. Within the scope of preliminary design activities, the initial sizing, optimizations and performance analyzes of the components were made. By using these results of the design, it was observed that the number of design iterations and the design time were significantly reduced.

### Keywords

Unmanned Aerial Vehicle (UAV)  
 Product Design  
 Optimization  
 Cargo Transportation  
 Quadrotor

### Time Scale of Article

Received 15 July 2023  
 Revised to 6 September 2023  
 Accepted 22 September 2023  
 Online date 30 December 2023

## 1. Introduction

Unmanned aerial systems are devices that can effectively carry out numerous missions in both military and civilian domains due to their diverse payload capacities, various performance features, and cost-effective operation. These tools are increasingly preferred across various fields such as agriculture and photography as a replacement for human labor. With their robust autonomous flight capabilities, high mobility, low cost, and fuel efficiency, drones are increasingly utilized in active and complex offensive applications. These applications include meteorological studies, photography, air cargo transport, forest fire detection, search-rescue operations, and it is

anticipated that new areas for drone utilization will emerge in the coming years.

In recent years, the advancement of unmanned aerial vehicles (UAVs) has led to the emergence of cargo drones as an innovative solution for logistics and transportation (Pugliese et al, 2020). These unmanned vehicles have the potential to change the way goods are transported, offering faster, more efficient, and environment friendly delivery options. Cargo drones, also known as delivery drones, are autonomous or remotely piloted vehicles specifically designed to transport goods (Jeongeun et al, 2019). These aerial vehicles use advanced navigation systems, sensors, and artificial intelligence algorithms to ensure safe and precise delivery operations. They can carry payloads ranging from small packages such as

\*: Corresponding Author Fikret Kamil Corbaci, [fikretkamil.corbaci@gmail.com](mailto:fikretkamil.corbaci@gmail.com)  
 DOI: [10.23890/IJAST.vm04is02.0202](https://doi.org/10.23890/IJAST.vm04is02.0202)

official document to heavier loads, depending on their design and capabilities.

Cargo drones have a huge potential to significantly reduce delivery times, especially in urban areas with congested road networks (Elouarouar and Medromi, 2022). By bypassing traffic and taking direct aerial routes, drones can swiftly transport goods, enabling rapid delivery and enhanced customer satisfaction. Compared to traditional highway delivery methods, cargo drones can offer cost savings by eliminating the need for human drivers, reducing fuel consumption, and optimizing delivery routes. These savings can potentially translate into more affordable and accessible goods for consumers. Furthermore, with the growing concerns over carbon emissions and environmental impact of it, cargo drones present a green alternative to traditional transportation. By relying on electric, drones produce fewer greenhouse gas emissions, contributing to more sustainable future.

Cargo drones also have an opportunity to reach remote and inaccessible areas that do not have adequate infrastructure, such as islands, rural areas, or disaster regions. This accessibility can ensure fast delivery of necessary supplies, medical aid, and humanitarian assistance.

When it comes to practice, cargo drones have some difficulties and limitations in terms of regulation, range, and cargo capacity. The adoption of cargo drones faces regulatory challenges related to airspace management, safety, and privacy concerns (Ahirwar et al, 2019). Governments and aviation authorities need to develop comprehensive frameworks to address these issues, ensuring the safe integration of drones into existing airspace management systems.

While cargo drone technology continues to advance, limitations still exist regarding payload capacity and range. Larger and heavier deliveries require more robust drones with longer flight endurance. Overcoming these technical constraints is crucial for the integration of cargo drones into logistics operations.

In addition, delivery operations can be affected by adverse weather conditions, such as strong winds, rain, fog, which may impact flight safety and efficiency. Developing drones with improved weather resistance and navigation capabilities is essential for their reliability and scalability.

Cargo drones, which continue to evolve despite limitations and challenges, have the potential to make a significant impact in many different areas. Cargo drones can revolutionize the e-commerce industry by offering same-day or even same-hour delivery options. This can improve customer satisfaction, reduce shipping costs, and enable businesses to expand their operations. Cargo drones also have the potential to revolutionize

healthcare logistics by delivering medical supplies, vaccines, and even organs for transplantation in a timely and efficient manner. They can also support emergency services by rapidly transporting critical equipment or providing situational awareness in disaster areas.

## 2. Method

To have an optimal Cargo UAV preliminary design, mission profile-based requirements should be guided during the design process. In order to achieve optimized design solutions, flight time inefficiency, losses in payload capacity, time and cost losses, etc. should also be taken into account and the design process should be carried out step by step.

It can be mentioned that quadcopter design and performance analyses related activities are divided into four subtitles as conceptual design for quadcopter frame geometry selection and frame sizing, gross take off weight (GTOW) optimization (Winslow et al, 2018), electronic component selection, and flight performance analyses at the last step.

After determination of frame geometry and frame sizing, focus was increased onto optimization of GTOW development of a by using a parametric approach which was proposed at our previous research (Corbaci and Dogan, 2023). The parameters related to the weight of Quadrotor were already determined as thrust and maximum continuous current, battery capacity, propeller diameter and frame size at previous study. These are used as the basic parameters on which the system features of the Cargo UAV depend throughout the study.

As given Flowchart at Fig.1, first of all, we obtained the main design inputs and checked them if they were consistent. After getting them, we determined the initial frame size and material type to optimize the strength of the quadrotor structure. Next, in order to get maximum thrust, we start to iteration and estimate the initial GTOW using the parametric approach with the help of the parameters selected above. We perform the selection of motor by using maximum thrust parameter, the selection of propeller by using propeller diameter parameter and battery selection by using cell number and capacity parameters.

Thus, so in the final step of iteration, the total weight, including cargo and avionics, is revealed. We need to decide whether to continue the iteration by carrying out a performance CFD analysis of the UAV, whose carrier body, subsystems used and weights have been revealed.

If it turns out that we don't need to drive the iteration, we can assume that the preliminary design of the drone is obtained. Although our work was in the preliminary design phase, we also checked whether we were

progressing on a competitive concept by estimating the cost. In this way, we gained the opportunity to make

changes on the selected components.

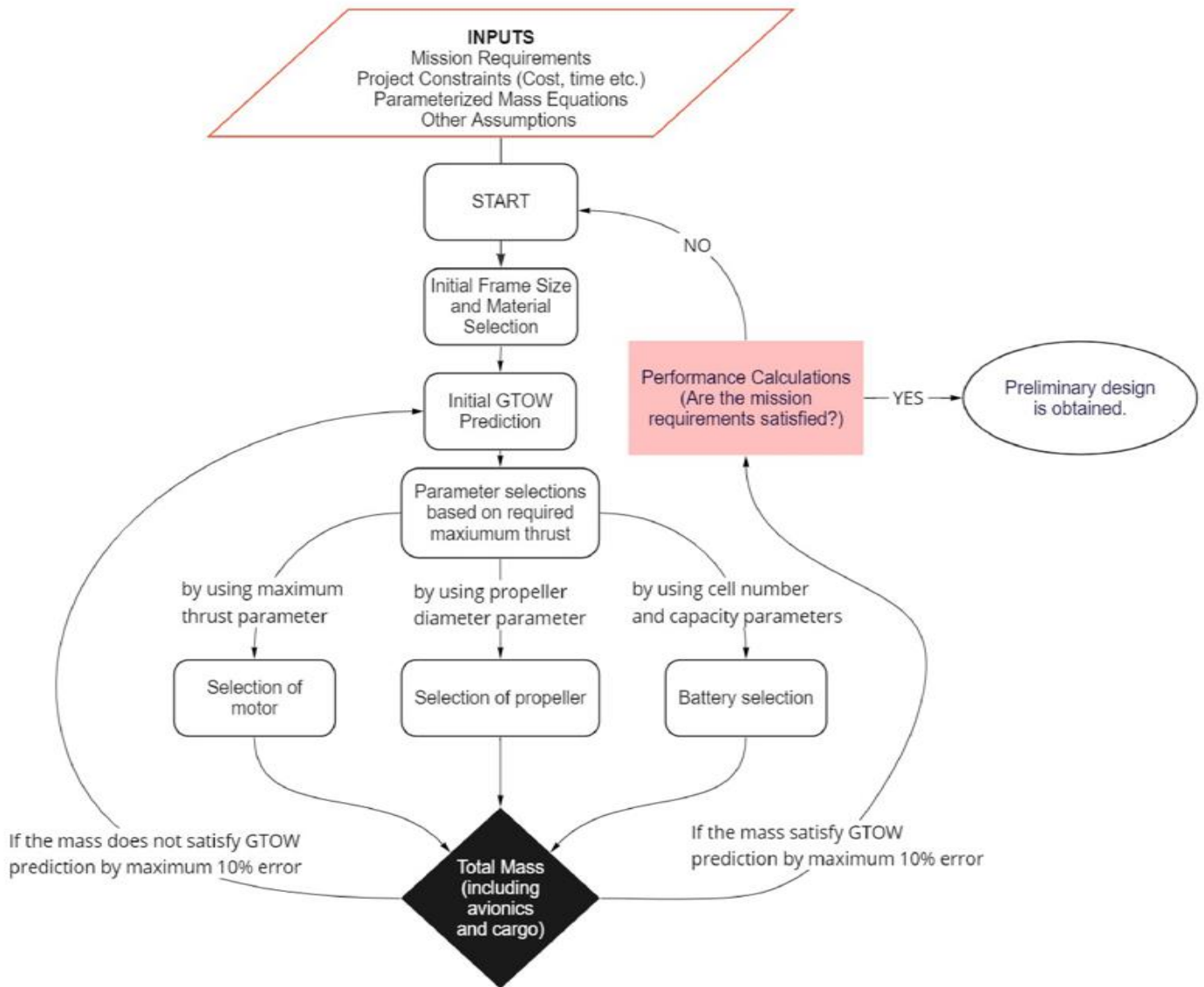


**Figure 1.** Flowchart of the iterative activities to obtain preliminary design of UAV

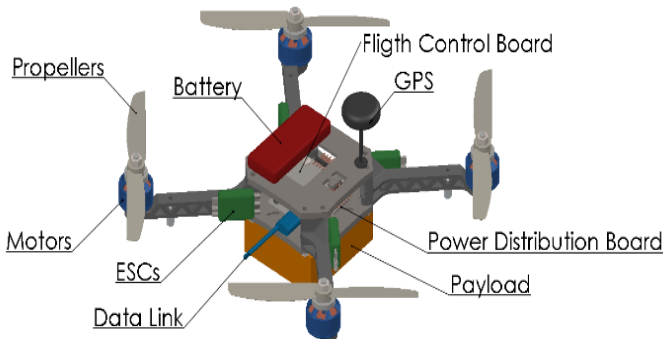


**Figure 2.** Fundamental subsystems of a quadrotor UAV

After the parameters of the final product are determined in the Preliminary Design Phase, the relevant systems, subsystems and components are maturely selected as represented in Figure 2.

Related component requirements were obtained from mission requirements and design features that meet these requirements were created compatibly. By using this component allocation, Cargo UAV System Chart was established for determined design features and presented at Fig.3.

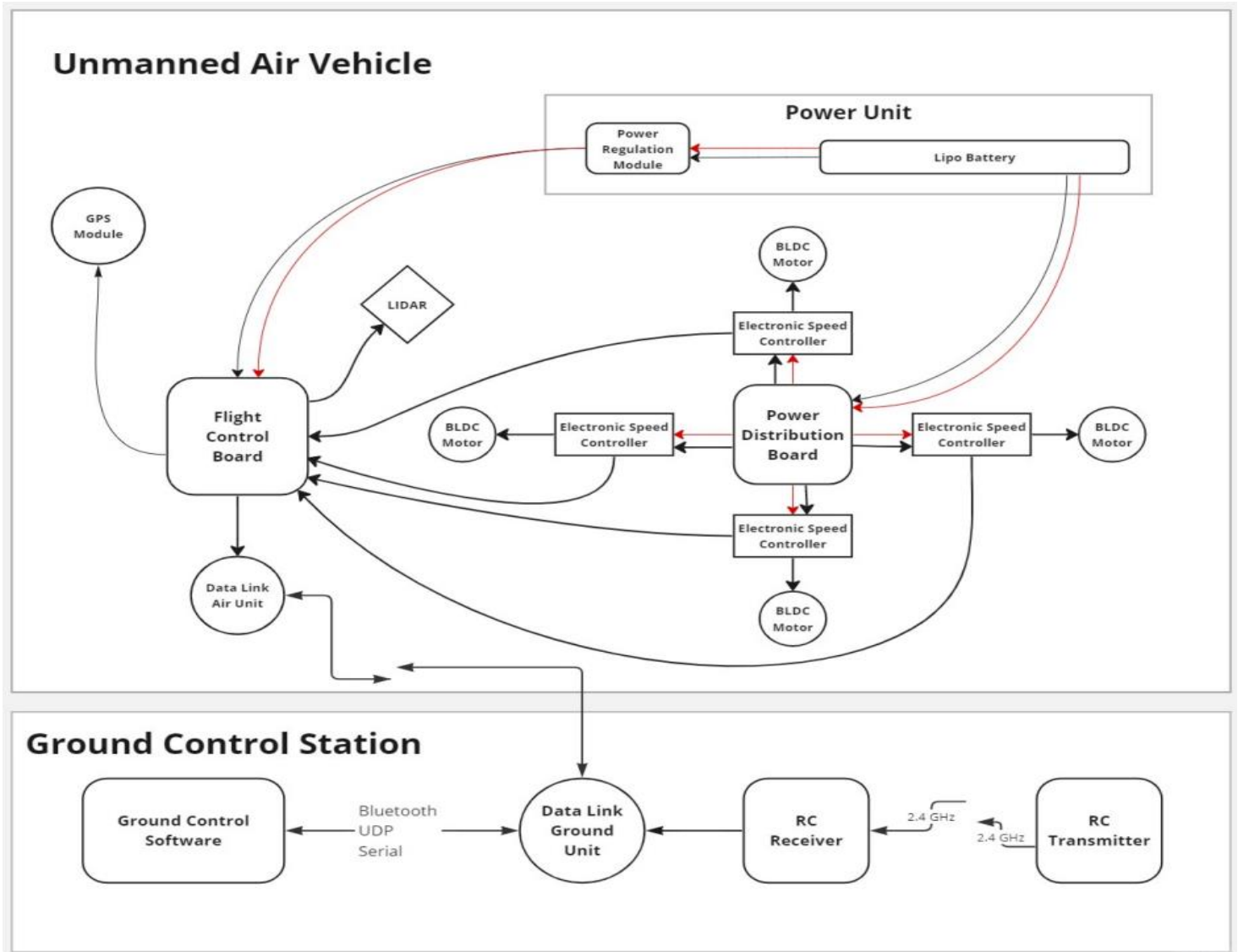


**Figure 3.** System Chart of the quadrotor UAV

**2.1. Mission Profile**

It is aimed to design a quadcopter which is used for local air cargo transportation in small urban areas and on-campus deliveries. The distance in between two delivery points are foreseen as approx. 1,500 m. The load to be carried by the vehicle consists of authentic documents that have maximum 200 g weight. In a single delivery, the drone takes off, climbs to the lowest altitude of 40 m and moves at cruising speed towards the delivery point. When it reaches the delivery point, it lands and stops the engines for safety. With the completion of the delivery, the drone rises to an altitude of 40 m again and returns to the starting point for the next delivery to be loaded. It is assumed that the quadrotor has  $3.44 \text{ m/s}^2$  acceleration at starting point and  $-1.67 \text{ m/s}^2$  deceleration at target point. And all other information for flight plan of the UAV are given at Fig.4 in detail.

**2.2. Mission Requirements**

After the preliminary evaluation for the determined mission profile, the basic mission requirements of the unmanned aerial vehicle were determined as in the Table.1. These mission requirements are considered as benchmarking values during design evaluation.

**Table 1.** Minimum performance requirements

No	Requirement	Value
1	Average Cruise Velocity	5 m/s
2	GTOW	12.5 N
3	Minimum Flight Time	10 min
4	Payload Capacity	0.200 kg
5	Communication Range	1,500 m
6	Mass of Avionics	0.200 kg

Other important assumptions related to quadrotor UAV design could be mentioned as ABS material will be used; it will consist of 2 plates, upper and lower and have true-X geometry.



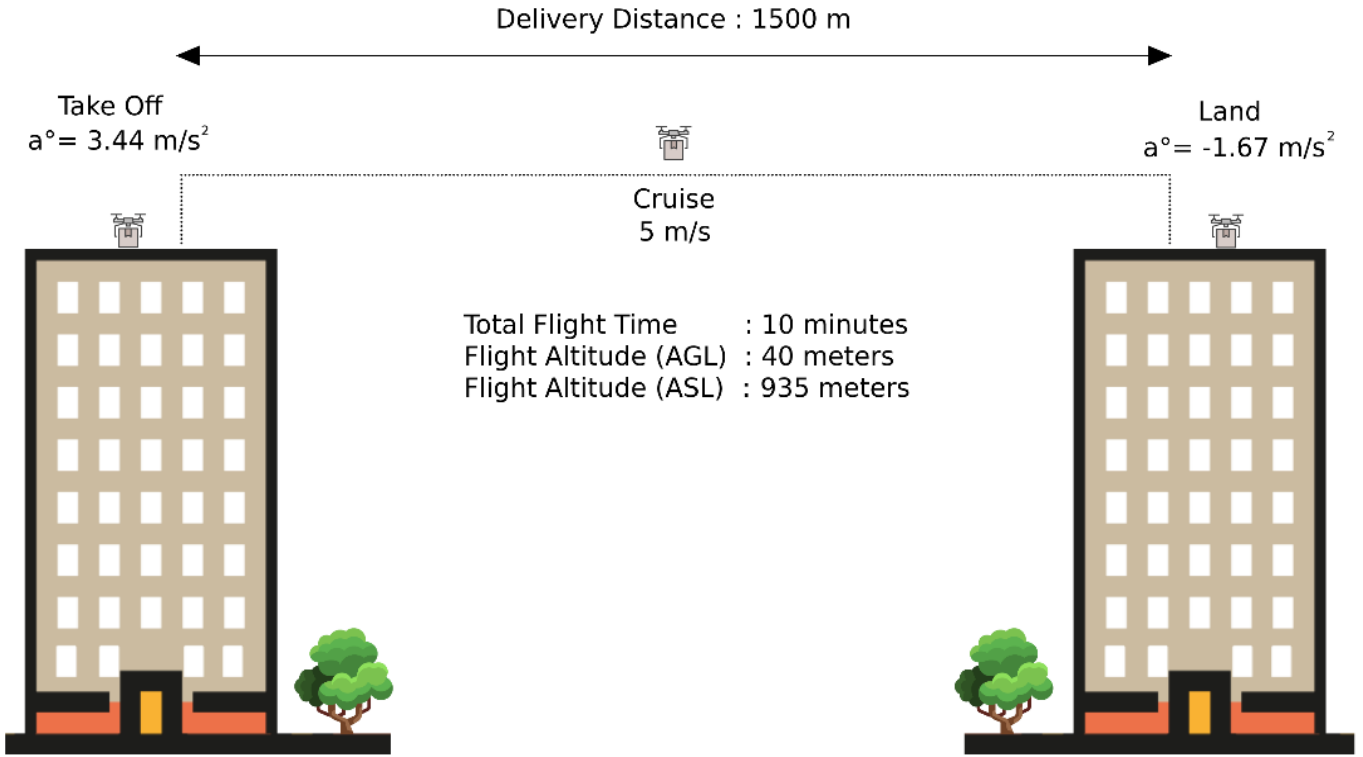


**Figure 4.** Flight Plan of the Quadrotor UAV

### 3. Preliminary Design of Quadrotor UAV

#### 3.1. Determination of Initial GTOW

To start the design iteration, first of all, we have to determine an initial GTOW. In our previous study a regression analysis based approach was proposed successfully (Corbaci and Dogan, 2023). According to this approach, the masses of the components should be calculated primarily in order to see that it can perform the expected performance in the targeted mission specifications. One of the most important design inputs to determine the masses of the components at this stage is the Cargo UAV Gross Take Off Weight (GTOW). It is assumed that GTOW consists of the masses [g] of the engine ( $m_m$ ), ESC ( $m_E$ ), battery ( $m_B$ ), propeller ( $m_p$ ), frame ( $m_f$ ), avionics ( $m_A$ ) and payload ( $m_{PL}$ ), which are the main components in the UAV.

$$GTOW = (m_m + m_E + m_B + m_p + m_f + m_A + m_{PL}) \cdot g \text{ [N]} \quad (1)$$

In the preliminary design, it is necessary to determine the initial GTOW which will be created by the preliminary estimate of the mass to be revealed for each of the components. All relevant component masses were separately determined with respect to predetermined parameters for each component by using regression analyses. While doing this, the tables prepared for the product alternatives that are sold commercially for each component and containing catalog data about both mass and the relevant parameter were used. When the payload changes, this initial value is re-estimated and

iteration continues accordingly.

The equations that emerged after the regression analyzes were formed as follows:

A. Mass of Motor ( $m_m$ ) with respect to Maximum Thrust of Motor ( $T$ ):

The weight of a BLDC motor can be parameterized by Maximum Thrust of Motor ( $T$ ) since the more thrust requires more power, then bigger size and higher mass. It may be established a linear correlation between Mass of Motor ( $m_m$ ) and Maximum Thrust of Motor ( $T$ ) available in the market, as shown in Fig.5 and Eq.2

$$m_m = 1E - 07(T)^3 - 0.0003(T)^2 + 0.2783(T) - 56.133 \text{ [g]} \quad (2)$$

B. Mass of ESC ( $m_E$ ) with respect to Maximum Continuous Current of ESC ( $I_{max}$ ):

According to the study with 55 different ESCs produced by various manufacturers, Mass of ESC ( $m_E$ ) is linearly parameterized by using their Maximum Continuous Current of ESC ( $I_{max}$ ) as shown in the Fig. 6 and Eq. 3

C. C. Mass of the Battery ( $m_B$ ) with respect to Capacity of the Battery ( $C$ ) and number of cells:

Mass of the Battery ( $m_B$ ) can be parameterized by cell numbers of 3, 4, and 8 and Capacity of the Battery ( $C$ ) as shown in the Fig. 7 and relevant equations for 3, 4, and 6 cell numbers are given in equations 4, 5 and 6 respectively.

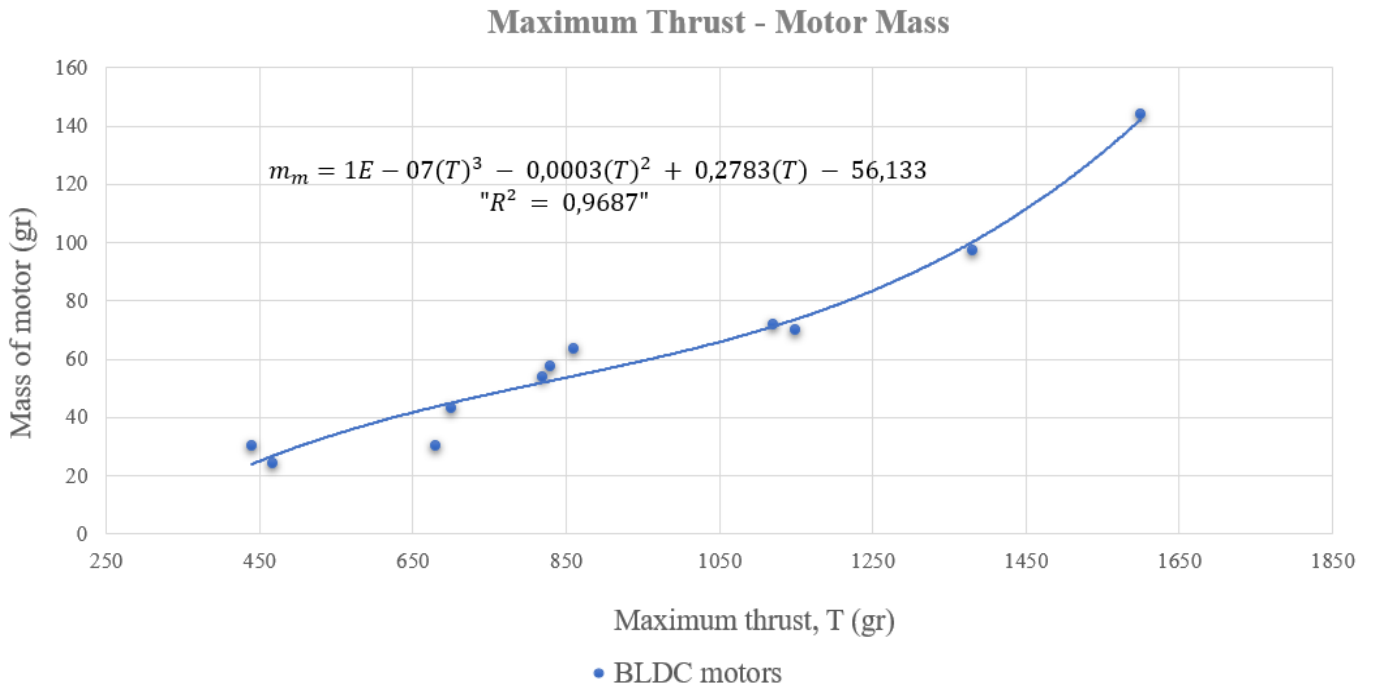


Figure 5. Mass of Motor ( $m_m$ ) with respect to Maximum Thrust of Motor ( $T$ )

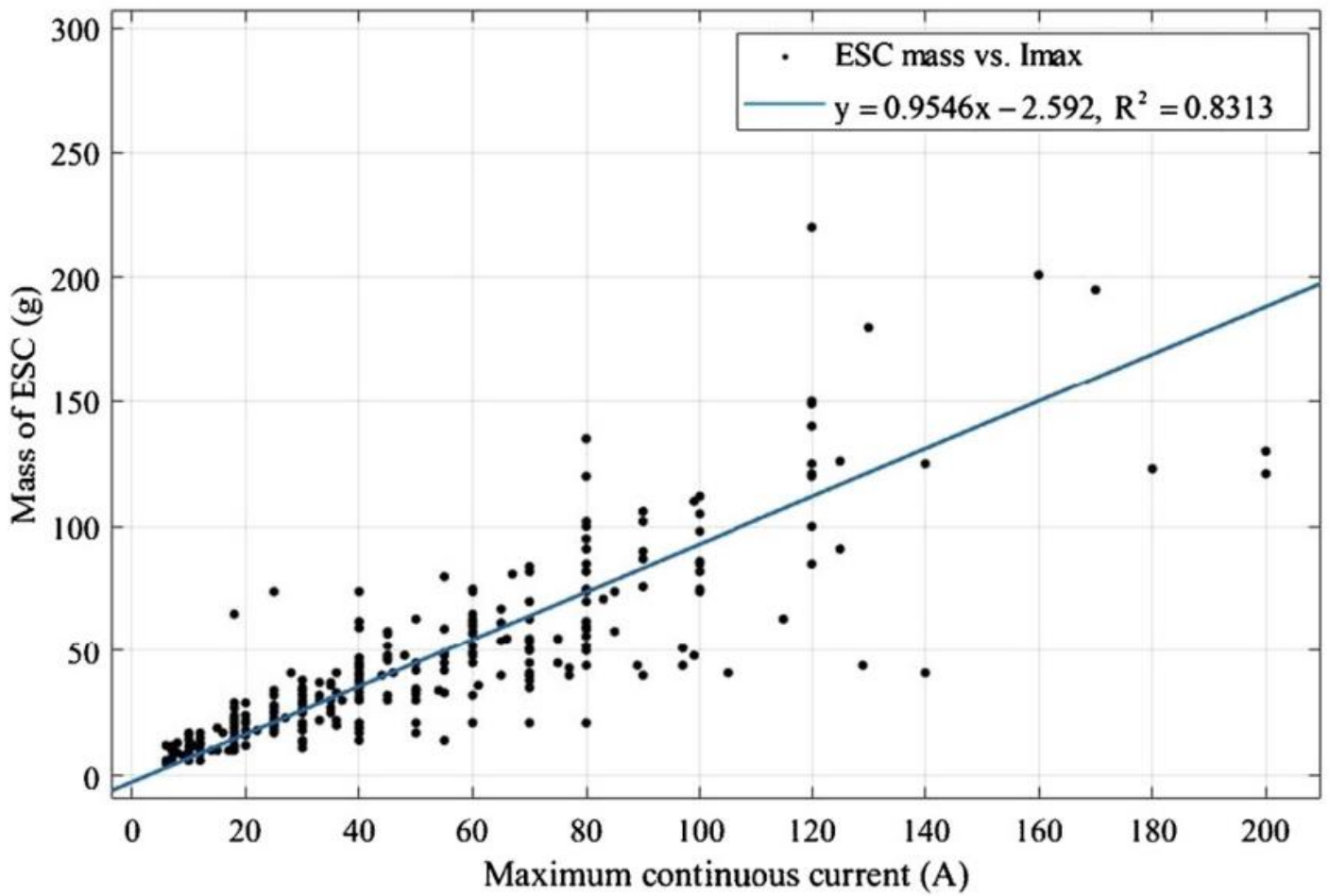


Figure 6. Mass of ESC ( $m_E$ ) with respect to Maximum Continuous Current of ESC ( $I_{max}$ ), (Vu NA et al, 2019)

$$m_E = 0.9546(I_{max}) - 2.592 [g] \quad (3) \quad \text{For } n=4, m_B = 0.761(C) + 69.522 [g] \quad (5)$$

$$\text{For } n=3, m_B = 0.0625(C) + 35.526 [g] \quad (4) \quad \text{For } n=6, m_B = 0.1169(C) + 132.0 [g] \quad (6)$$

D. C. Mass of the Battery ( $m_B$ ) with respect to Capacity of the Battery ( $C$ ) and number of cells:

Mass of the Battery ( $m_B$ ) can be parameterized by cell numbers of 3, 4, and 8 and Capacity of the Battery ( $C$ ) as shown in the Fig. 7 and relevant equations for 3, 4, and 6 cell numbers are given in equations 4, 5 and 6 respectively.

E. Mass of the Propeller ( $m_p$ ) with respect to Diameter of the Propeller ( $d_p$ ):

Mass of the Propeller ( $m_p$ ) for more than 50 carbon fiber propellers in UIUC database can be parameterized in terms of Diameter of the Propeller ( $d_p$ ) as shown in Fig.8 and Eq.7.

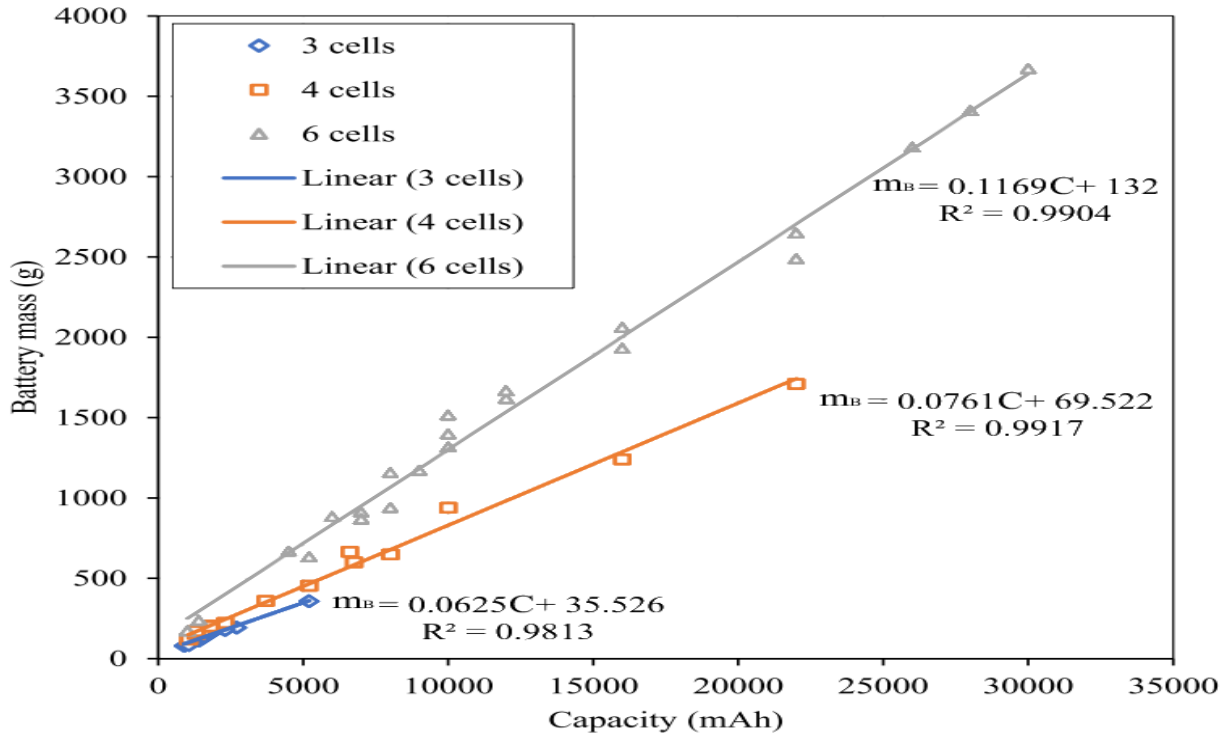


Figure 7. Mass of the Battery ( $m_B$ ) with respect to Capacity of the Battery ( $C$ ), (Vu NA et al, 2019)

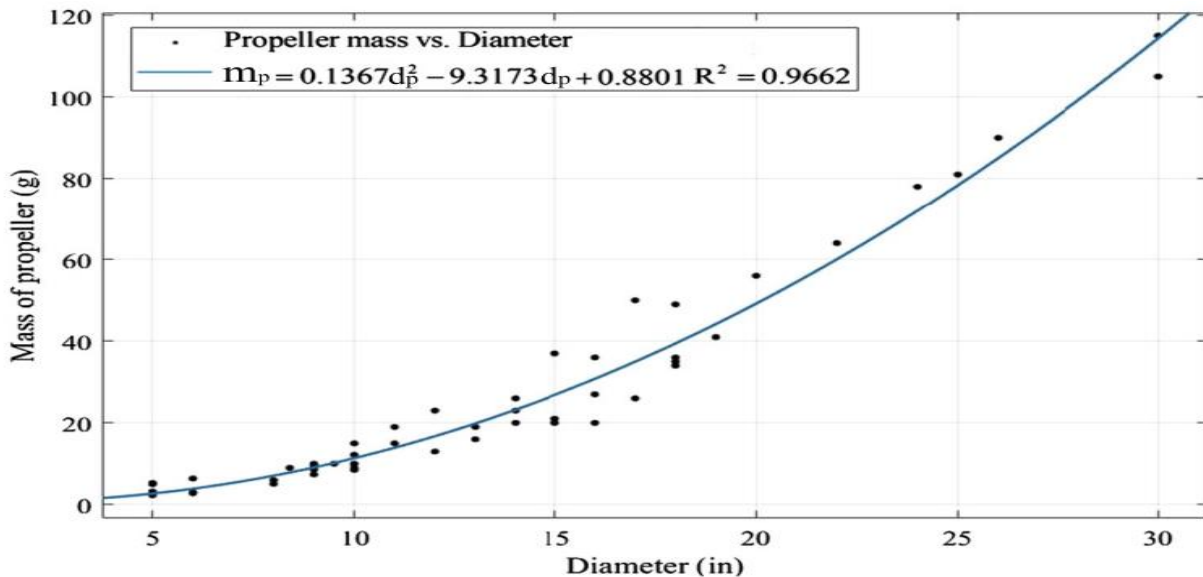
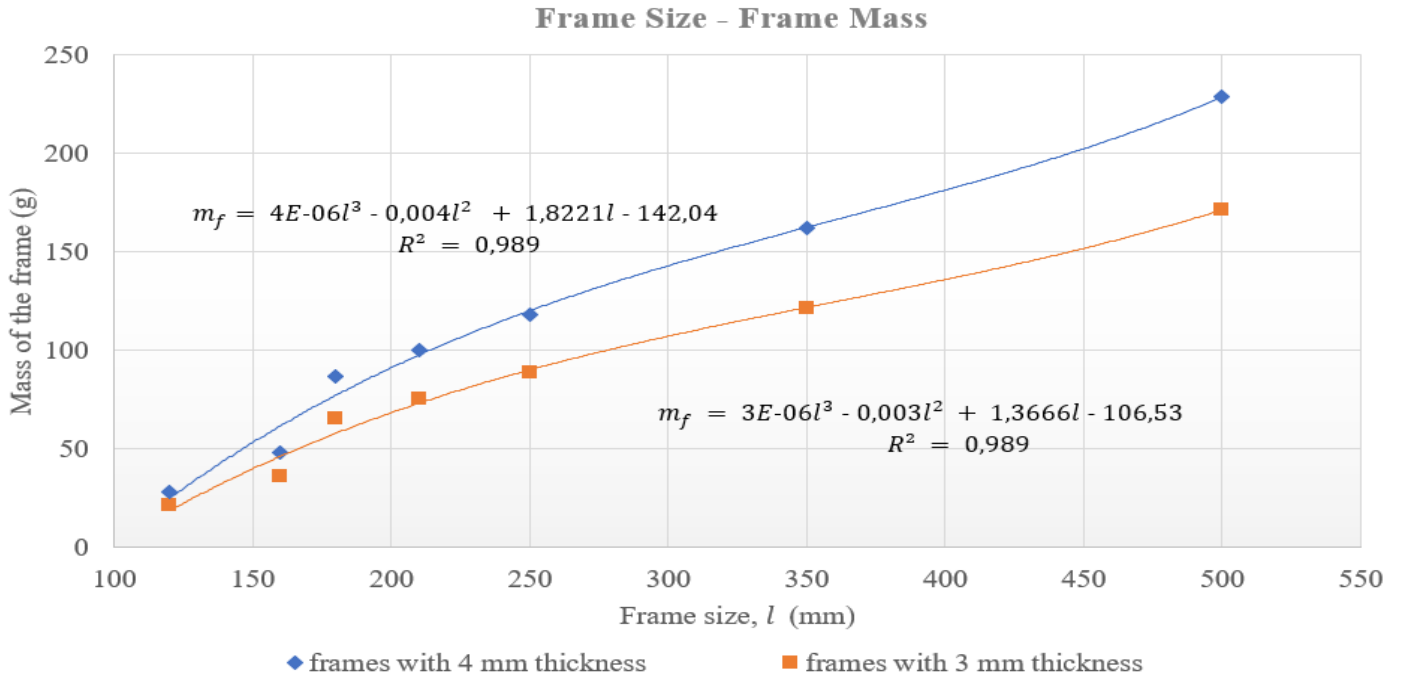


Figure 8. Mass of the Propeller ( $m_p$ ) with respect to Diameter of the Propeller ( $d_p$ ), (Vu NA et al, 2019)

$$m_p = 0.1367(d_p)^2 - 9.317(d_p) + 0.881 \text{ [g]} \quad (7)$$

F. Mass of the Frame ( $m_f$ ) with respect to Diagonal Size of the Frame ( $l$ ) and Thickness ( $t$ ):

Mass of the Frame ( $m_f$ ) is correlated linearly with respect to Diagonal Size of the Frame ( $l$ ) and with 3 mm and 4 mm Thickness ( $t$ ) and selected ABS material with density of averagely  $1.04 \text{ kg/m}^3$ . The results are given in Fig.9 and Eq.8 and Eq.9 respectively.



**Figure 9.** Mass of the Frame ( $m_f$ ) with respect to Diagonal Size of the Frame ( $l$ ) and Thickness ( $t$ )

For  $t=3mm, m_f = 3E - 06(l)^3 - 0.003(l)^2 + 1.3666(l) - 106.53 [g]$  (8)

For  $t=4mm, m_f = 4E - 06(l)^3 - 0.004(l)^2 + 1.8221(l) - 142.04 [g]$  (9)

Thus, initial GTOW was determined as a function of all selected parameters.

$$GTOW = f(T, I_{max}, C, n, d_p, l, t) [N] \quad (10)$$

This initial GTOW (Eq.10) found will be used in the preliminary design of all components, and the necessary selections are easily completed as follows. As a result of the regression analysis and initial GTOW determination, the overall mass profile of the quadcopter is obtained. Based on the GTOW, required thrust values and propulsion system components are selected. Then, based on the propulsion system and frame weights, expected air cargo and payload capacities are corrected. GTOW including payloads were assumed as 12.50 N to calculate initial required thrust for each motor.

In the following sections, based on the initial GTOW (12.50 N) determined up to this point, performance analyses of the quadcopter are made in order to determine whether a second iteration of sizing is needed.

#### 4. CFD Analyses and Performance Evaluations

Aerodynamic performance of the propellers of a quadcopter has considerable impact on quadcopter overall performance. Aerodynamic performance of a propeller can be defined in terms of some unitless parameters that are thrust coefficient ( $C_T$ ), power coefficient ( $C_P$ ), advance ratio ( $J$ ), and propeller efficiency

( $\eta$ ). (McCormic, 1994). The parameters are defined as follows:

$$C_T = \frac{T}{\rho \times n^2 \times D^2} \quad (11)$$

$$C_P = \frac{P}{\rho \times n^3 \times D^5} \quad (12)$$

$$J = \frac{V}{n \times D} \quad (13)$$

$$\eta = J \times \frac{C_T}{C_P} \quad (14)$$

where  $n$  is the rotational speed in revolutions per second and  $D$  is the propeller diameter (McCormic, 1994). Thus, thrust and power coefficients are functions of advance ratio, accordingly, Reynolds number and geometry of the propeller (Brandt and Selig, 2011). Reynolds number of the propeller is calculated based on the propeller chord at the 75% propeller blade-station (Brandt and Selig, 2011).

$$C_T = f(J, Re, \text{propeller geometry}) \quad (15)$$

$$C_P = f(J, Re, \text{propeller geometry}) \quad (16)$$

Computational fluid dynamics (CFD) analysis is performed to examine thrust performance of the propeller according to various airspeed and rotational speed values (Kutty and Rajendran, 2017). As a steady-state approximation, the Multiple Reference Frame (MRF) approach is applied to simulate rotation of the propeller without rotating mesh.

In the pre-processing step, the propeller geometry that is created in the Solidworks CAD software is imported the ANSYS Workbench Software. The computational domain is created as a static cylindrical zone and a rotating cylindrical subzone in it. The boundaries of the



zones are adjusted in sufficient dimensions based on the thickness studies (Stajuda et al, 2016) not to adversely affect the flow. Also, very large sizes are avoided to not to prolong the analysis time. The dimension of the computational domain is given in Fig.10.

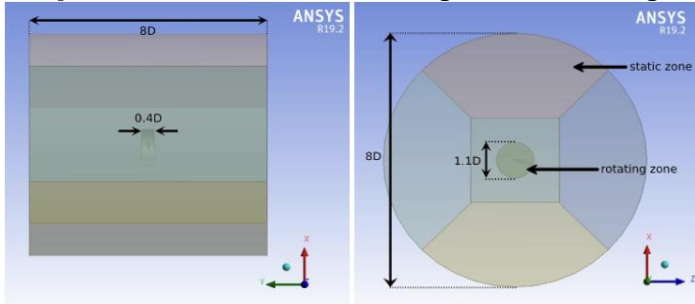


**Figure.10** Computational domain dimensions from side and front views.

**Table 2.** Boundary Conditions

Boundary Name	Condition	Turbulence Intensity
Inlet	1 Atm static pressure and $V_{\infty} = 0 \text{ m/s}$	1%
Outlet	1 Atm static pressure	1%

**Table 3.** Propeller performance results (Propeller Thrust and Power Coefficients)

rpm	Re	$C_T^*$	$C_P^*$	$C_T^{**}$	$C_P^{**}$	$C_T^{***}$	$C_P^{***}$
4008	21e03	0.1161	0.0481	0.0817	0.0337	37.7%	35.2%
4500	23e03	0.1171	0.0481	0.0819	0.0336	35.3%	35.5%
5013	26e03	0.1176	0.0482	0.0821	0.0336	35.5%	35.7%
6500	33e03	0.1194	0.0482	0.0825	0.0333	36.5%	36.5%

\*Experimental Results, \*\*CFD Results

When the difference between numerical results and experimental results are examined, it is obviously seen that a significant difference is occurred. Increases in the rpm values cause consistent increases in the thrust coefficient and hence the thrust force increases. Also, it should not be neglected that the flow over a propeller is highly complex, it may require to run a transient analysis by expecting more accurate values with contrast to a steady-state analysis. By using transient analysis,

The computational domain is discretized by using ANSYS Fluent with the maximum skewness of 0.8 and minimum orthogonal quality of 0.2.

Two boundary conditions are set in solver step as shown in the Table 2. The inlet boundary condition describes the entrance of flow, and the outlet boundary condition describes exit of the flow. Cell zone condition setup is adjusted to the rotational speed values of the propeller for frame rotation.

The turbulence model is selected as  $k-\omega$  SST model. In computational fluid dynamics, the  $k-\omega$  turbulence model is a common two-equation turbulence model that is used as an approximation for the Reynolds averaged Navier–Stokes equations (RANS).

In the post-processing step, the thrust forces, pressure on the propeller, velocity streamlines, and volumetric renders of rotating computational domain with respect to several rpm values are compiled and visualized. Thrust and power coefficient results obtained by CFD analysis and experimental results are given in the Table 3.

dynamic mesh approach is can be used to simulate rotation of the propeller more accurately.

Further, when it is checked the pressure contour given in the Fig.11 and Fig.12, the thrust generation by the pressure gradient between propeller surfaces (upstream and downstream of disc) can be seen. Also, an increase in the pressure gradient with respect to increasing rotational velocity is expected.

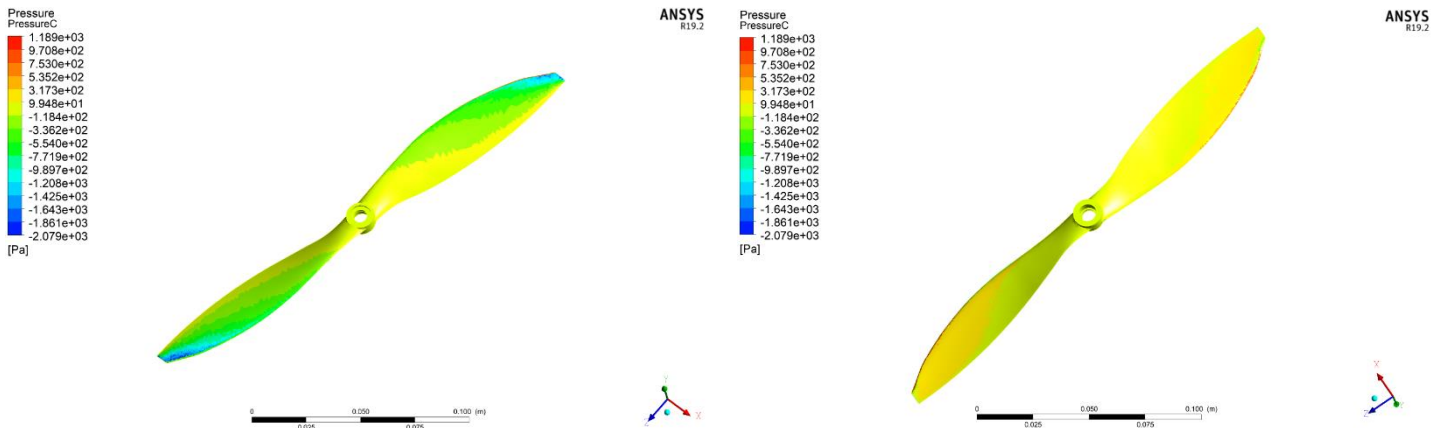


**Figure 11.** Pressure contour of the propeller a) front surface b) and back surface at 4008 rpm.

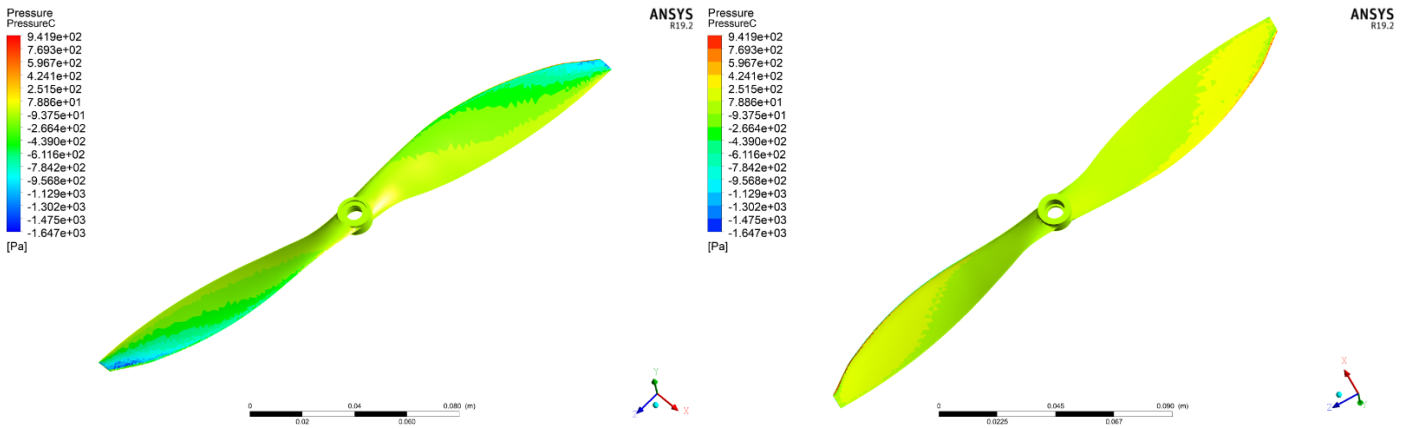


**Figure 12.** Pressure contour of the propeller a) front surface and b) back surface 4500 rpm.

Fig.13 and Fig.14 represent the forward velocity streamlines of the propeller in view of XY plane for 4008 and 6500 rpm values. It is clear from the figures that the velocity of the air in the rotating zone increases as the rotational velocity increases. The propeller induces a rotational velocity and accelerates air. As the rotational velocity of the propeller increases, the speed of air passes the propeller increases.

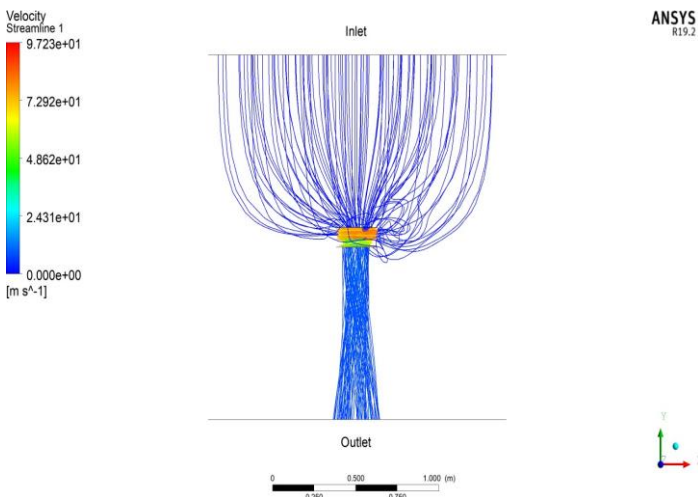


**Figure 13.** Forward velocity profile of computational domain at 4008 rpm.

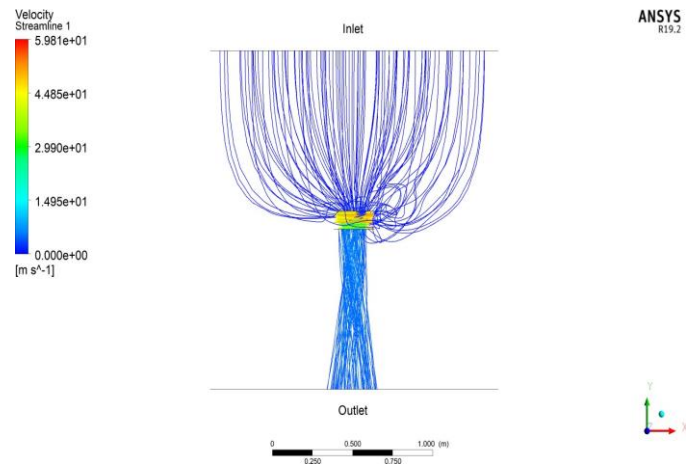


**Figure 14.** Forward velocity profile of computational domain at 6500 rpm

### 5. Results and Discussion

Preliminary design activities were carried out in order to provide the mission requirements selected based on the mission profile of the Cargo quadrotor UAV. Reducing the design iteration times within the scope of these activities will make a significant contribution to the designers. In the study, the focus is on pre-determining the components in the UAV at the Preliminary design stage and specified in Fig.3 with the current selection parameters and checking the required performance qualifications according to the weight of the UAV that will emerge after this selection. For this, the values that will ensure its performance in the take-off phase, and especially the Gross Take Off Weight (GTOW) should be taken into account, as the usage phase expected to show the highest capability from the UAV. However, in doing so, we need a systematic approach to find an accurate value and take it into account. We take this approach in the form of regression with the parameters that we will choose in all components to reach the initial GTOW. In this study, regression analyzes put forward in this way are detailed. For each component type, different existing products were examined, and a regression was created between the important basic parameters and component weight values. For some components, the values found in the literature have been taken into account. Thus, the initial GTOW calculation has been completed with the approaches created for all relevant component groups.

Thanks to the initial GTOW found, it is possible to make the first iteration of the design. After this stage, the preliminary design iteration continues by examining the effect of the resulting GTOW value on the selected components until the specified acceptable levels are reached. A comparison was made between the GTOW obtained as a result of the final component selections within the scope of the preliminary design, which emerged after these processes, and the initial GTOW obtained from the estimation regression approach as given at Table 4.

**Table 4.** Calculated mass compared to solution design mass based on selections

No	Component	Calculated Mass [g]	Solution Design Mass [g]	%Difference	Share-Calc %	Share-Act %
1	Motor (x4)	100.52	234.00	132.8%	8%	17%
2	Frame	162.25	252.80	55.8%	13%	19%
3	Battery	248.00	255.00	2.8%	20%	19%
4	Propeller (x4)	64.00	36.00	-43.8%	5%	3%
5	ESC (x4)	104.20	148.00	42.0%	8%	11%
6	Avionics	371.00	234.10	-42.3%	30%	16%
7	Air Cargo	200.00	200.00	-	-	-
8	TOTAL	1,250.00	1,359.90	8.8%		

## 6. Conclusions

After the comparison, it was observed that the success rate of the GTOW estimation regression approach presented in the study was at a reasonable level. With this method, it has been observed that the design iterations, which yielded results in a high level of compliance with the mission requirements, were carried out in shorter time periods.

It may be useful to mention the issues that can be addressed in the future as additional studies. In this context, after the approach used in this study, a structure can be created in which the resolution of the analyzes and calculations taken into account for the design iteration can be controlled. In addition, it would be beneficial to conduct additional trials with more effective alternatives such as Coupled analysis, with emphasis on diversification of performance analysis.

## Nomenclature

UAV	: Unmanned Aerial Vehicle
GTOW	: Gross Take of Weight
ESC	: Electronic Speed Controller
GPS	: Global Positioning System
LIDAR	: Laser Imaging Detection and Ranging
$g$	: Gravitational Constant
CFD	: Computational Fluid Dynamics
BLDC	: Brushless Direct Current

## CRediT Author Statement

Both authors committed that this statement page reflects an accurate and detailed description of their diverse contributions to the proposed Article as follows; **Fikret Kamil Corbaci**: Conceptualization, Methodology, Writing – Original Draft, Supervision, Writing – Review & Editing, Validation. **Yunus Emre Dogan**: Writing – Original Draft, Visualization, Investigation, Formal Analysis

## References

- Ahirwar, S., Swarnkar, R., Bhukya, S. and Namwade, G. (2019). Application of drone in agriculture. *International Journal of Current Microbiology and Applied Sciences*, 8(01), pp.2500-2505. <https://doi.org/10.20546/ijcmas.2019.801.264>
- Brandt, J. and Selig, M., (2011). January. Propeller Performance Data at Low Reynolds Numbers. In 49th AIAA Aerospace Sciences Meeting including the New Horizons Forum and Aerospace Exposition (p. 1255). <https://doi.org/10.2514/6.2011-1255>
- Corbaci, F.K. and Dogan, Y.E., (2023), Parametric Approach To Initial Weight Determination At Preliminary Design Of A Quadrotor Cargo UAV, ISUDEF '23 International Symposium on Unmanned Systems: AI, Design and Efficiency 2023, Sustainable Aviation.
- Elouarouar, S. and Medromi, H. (2022). Multi-Rotors Unmanned Aerial Vehicles Power Supply and Energy Management. *E3S Web of Conferences*, 336, p.00068. <https://doi.org/10.1051/e3sconf/202233600068>
- Jeongeun, K., Seungwon, K., Chanyoung, J. and Hyoungil, S. (2019). Unmanned Aerial Vehicles in Agriculture: A Review of Perspective of Platform, Control, and Applications. *IEEE Transactions and Journals*, Volume 4, 2016, pp.1-17. <https://doi.org/10.1109/ACCESS.2019.2932119>
- Kutty, H.A. and Rajendran, P., (2017). 3D CFD Simulation and Experimental Validation of Small APC Slow Flyer Propeller Blade. *Aerospace*, 4(1), p.10. <https://doi.org/10.3390/aerospace4010010>
- McCormick, B.W., (1994). *Aerodynamics, Aeronautics, and Flight Mechanics*. John Wiley & Sons. p.300.
- Pugliese, L.D.P., Guerriero, F. and Macrina, G. (2020). Using drones for parcels delivery process. *Procedia Manufacturing*, 42, pp.488-497. <https://doi.org/10.1016/j.promfg.2020.02.043>

- Stajuda, M., Karczewski, M., Obidowski, D. and Jóźwik, K., (2016). Development of A CFD Model for Propeller Simulation. *Mechanics & Mechanical Engineering*, 20(4):579-593.
- Vu NA, Dang DK, Dinh TL (2019). Electric propulsion system sizing methodology for an agriculture multicopter. *Aerospace science and technology*, 90:314-326.  
<https://doi.org/10.1016/j.ast.2019.04.044>
- Winslow J, Hrishikeshavan V, and Chopra I, (2018). Design methodology for small-scale unmanned quadrotors. *Journal of Aircraft*, 55(3):1062-1070.  
<https://doi.org/10.2514/1.C034483>